Characterizing Nominal Analog Signal Deformation on GNSS Signals

R. Eric Phelts, Todd Walter, Per Enge
Stanford University

ABSTRACT

Satellite-based navigation requires precise knowledge of the structure of the transmitted signals. Accurate knowledge of the shapes of the code correlation peaks is required to ensure no biases are introduced into the position solution. It is often presumed that all incoming ranging codes (e.g., C/A codes) are effectively ideal. However, nominal signal deformations—small distortions of the code chip shapes—can lead to ranging errors. Distortions which are created by satellite filter imperfections in particular, may cause errors that vary significantly with receiver filter characteristics and code tracking loop implementations. These analog signal deformations should be well-understood so that receiver performance meets user requirements.

This paper discusses a methodology for characterizing nominal analog distortions. First, it identifies a general approach for specifying the nominal limits for GNSS codes. Second, it leverages actual measured data from code chip (step) responses of several existing GPS SVs to determine practical performance bounds. Next, it develops a generalized filter model to simulate and further analyze these signals. Finally, it provides examples of the potential user range error implications of these specifications to potentially determine whether or not they should be modified. While this methodology is developed using GPS C/A codes, it is proposed as a practical approach for determining useful specifications on future GNSS codes as well.

BACKGROUND

Nominal signal deformations result from imperfections in the signal generation hardware. The modulation timing, transmission filter, and antenna characteristics (e.g., bandwidth, group delay response, etc.) often deviate from ideal. When the transition times of the signal are not as designed due to modulator imperfections, changes in the widths of the chips may occur. In addition, filtering, or band limiting, always introduces some amount of nominal analog distortion (e.g., overshoot and ringing) onto the transmitted codes. Any of these effects may lead to range errors.

Although differential corrections may be applied by a reference receiver, users generally do not have identical receiver characteristics. Accordingly, differential corrections cannot remove all of these errors for all users, and signal deformations may limit user ranging accuracy. Left unaccounted for, such distortions may also pose a threat to integrity. Such limitations are of particular concern to systems such as WAAS and LAAS (Wide and Local Area Augmentation Systems, respectively), which propose to safeguard the integrity of GNSS signals for many aviation users.

Signal Deformation Faults: ICAO Threat Model

Potential integrity threats posed by signal deformation faults were first to be addressed. The International Civil Aviation Organization (ICAO) adopted the current standard threat model for signal deformation failures in 2000. The ICAO threat model separately identified and modeled both digital faults and analog faults of the GPS C/A codes. (A detailed discussion of the ICAO threat model is provided in [1].)

Digital faults were conceived as an advance or delay of either the rising or falling edge of a C/A code chip. The effect was to create “dead zones” (i.e., plateaus) atop an ideal correlation peak. Analog faults were modeled as an underdamped second-order step response that had large overshoot and/or an extended oscillatory response—with frequency F_D (MHz) and damping parameter σ (MNepers/sec)—relative to an ideal code chip. These potentially lead to large amounts of correlation peak asymmetry. Either effect could potentially create code tracking errors that vary significantly as a function of receiver bandwidth, filter group delay, discriminator type, and correlator spacing.

Nominal Digital Distortion

Nominal (and faulted) digital distortion effects have been modeled and analyzed fairly extensively. Both were first

observed on the GPSII-4 SV19 in 1993 [2]. Using oscilloscope traces recorded at Camp Parks Army Base, it was initially measured as an offset in the zero-crossings of the C/A code chips relative to those of the P(Y) code. Much later, in 2004, digital distortions nominally present on the GPS C/A code for each of 32 SVs were measured as timing offsets from ideal code sequences [3]. Pini, *et al*. later measured these distortions on several GPS SV signals as offsets from the P(Y) transitions (as was done by Camp Parks in 1993) [4]. More recently, digital distortions have been analyzed for their potential to reduce tracking performance on modernized code modulations such as L5 and also for their potential to lead to timing biases between different signal modulations [5].

Nominal Analog Distortion

Nominal analog distortions have also been observed and discussed in the past. They too were present in the data measured at Camp Parks in 1993. Mitelman, however, provided the first high-resolution comparisons of the nominal step responses of GPS C/A codes in 2004 [3]. His results also showed the potential of a correlation between these responses and the satellite block types. In addition, these results revealed the large disparity between nominal analog performance and the closest-fitting second-order step response. These traces are plotted in Figure 1.

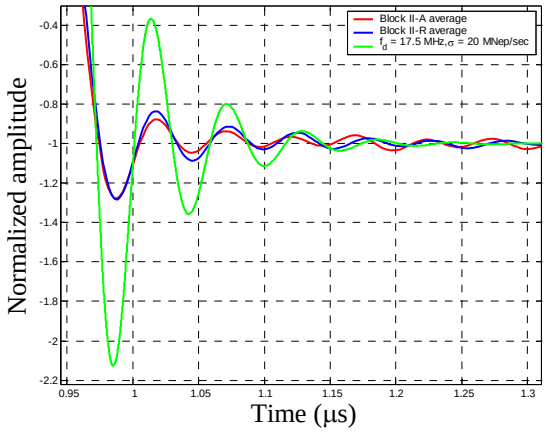

Figure 1. Comparison of nominal analog distortion on C/A code chips to a "best fit" ICAO threat model waveform. [3]

More timely measurements of nominal signal deformations are continually made by both WAAS and LAAS in real time. These systems employ multi-correlator receivers in their signal deformation monitoring (SDM) algorithms to reduce environmental noise and estimate the relative asymmetries of the C/A code correlation peaks. The monitors effectively measure the combined effects of analog and digital fault modes. Although a quantitative measure of any specific type of distortion is less clear, they provide an excellent means of evaluating the relative overall distortion of the GPS signals as they affect WAAS and LAAS users.

Figure 2 plots average monitor data for the WAAS detection metrics in October 2008 (10-day average). WAAS SDM measurements compare the deformations on any one SV signal to the median across the others [6]. The data indicates that the largest relative deformation occurs for PRN 23 (IIR-12, SVN60); PRN 11 (IIR-11, SVN59) had the second largest. (PRNs 33 and 34 in the figure correspond to estimates made on the WAAS GEOs.)

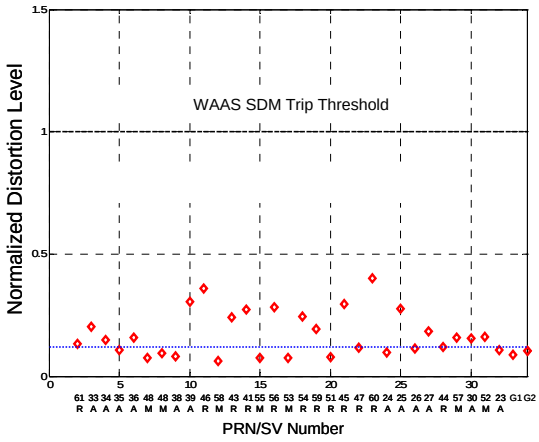

Figure 2. Nominal distortion summary data (October 2008, 10-day average) for all GPS SV and two WAAS GEOs as measured by the WAAS signal deformation monitor. (The SVN and the Block Type codes are provided on the horizontal axis below the PRN numbers.)

ANALYSIS AND RESULTS

To fully characterize analog signal distortions alone, the following procedure was employed:

1) Define the performance criteria for the nominal signals.
2) Determine the performance bounds of current nominal performance.
3) Model the nominal waveforms.
4) Determine the worst case nominal user receiver range errors.

1. Define Nominal Performance Criteria

Traditional transient system performance and "step" response analyses employ measures such as: Rise Time (t_R) (and/or Fall Time (t_F)), Peak Time (t_P), Settling time (t_S), and Peak Overshoot Ratio (POR). They are a practical means to analyze the nominal analog deformations for two primary reasons. First, they are intuitive measures of performance that can be used to characterize the responses of both second-order and

higher-order systems. Second, they have a well-established history of use in many different applications.

The definitions for each of these parameters as they apply to measured GNSS codes are as follows:

- An ideal code signal is the one that varies between -A and A instantaneously at a desired chip transition time, where A is the amplitude of the ideal signal.
- Peak Time (t_P) is the time it takes for the rising edge of the signal to rise from the preceding zero-crossing to its first maximum, or peak value.
- Rise Time (t_R) is the time it takes for the rising edge of the signal to increase from the preceding zero-crossing to the ideal amplitude +A.
- Fall Time (t_F) is the time it takes for the falling edge of the signal to decrease from the preceding zero-crossing to the ideal amplitude -A.
- Settling Time (t_S) is the time measured from the zero-crossing preceding a positive (or negative) chip to when the signal response first enters and then remains within a band whose width is computed as a percentage of amplitude for the remaining duration of the chip width.
- Peak Overshoot Ratio (POR) is given by the difference between the first peak height and the corresponding ideal code amplitude (A), divided by the ideal code amplitude (A). In Figure 3, POR = B/A.

Figure 3 illustrates each of these parameters on an ICAO analog waveform with a damped oscillation frequency (F_d) of 3MHz and an attenuation factor (σ) of 6MNepers/sec. (A full discussion of the equations used in these second-order waveforms is provided in [1].) The settling time amplitude variation depicted (5%) is for example purposes only.

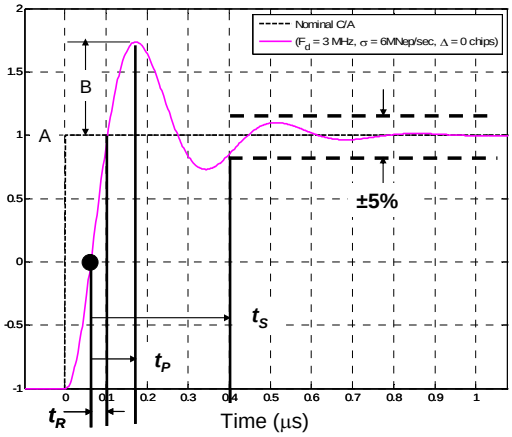

Figure 3. Transient "step" response performance criteria for a second-order waveform.

2. Determine Nominal Performance Bounds

Practical limits on the transient performance criteria can be determined by comparing the step responses of current, nominal GPS signals. In this paper, GPS C/A code measurements are discussed. However, a similar procedure can be followed for other GNSS signals. It is important to specify the measurement procedure so that meaningful comparisons of the signals can be made.

Although the performance criteria definitions may be unambiguous, the data collection methods and equipment, in addition to the normalization techniques used, may affect the derived performance parameter bounds. The methods used for this paper were selected for their practicality; however, they are not unique. Other methods may be equally as valid provided they permit consistent, repeatable measures of the signals that can be readily duplicated.

Measurement Processing

Four practical normalization procedures were defined for this analysis.

1) The ideal amplitude (A) is measured as the mean of the signal between the desired settling time (t_S) and 98% of the chip duration (to exclude the falling edge).
2) The chip selected for comparison from each SV was the chip corresponding to the largest POR. This defined the largest, and hence, most-limiting, condition on overshoot.
3) The transient responses for the selected chip were aligned at the zero-crossings for the rising edge. (Falling edges are not analyzed in this paper.)
4) The Settling Time requirement for the signals was fixed at 180ns and the settling amplitude was selected based on the data. The peak times and rise times were also selected based on the data.

The measurement equipment included a 47-meter parabolic dish antenna (owned and operated by Stanford Research Institute). This was used to take low-noise, low multipath measurements of the C/A codes transmitted by the current GPS satellites. High-bandwidth, high-resolution samples were recorded using an 89600 Agilent Vector Signal Analyzer. The effective sampling frequency (for the in-phase signal only) was 46.08MHz.

Doppler removal at each 1-ms code epoch was accomplished using a software-defined radio. Coherent averaging of each code epoch was limited to no more than two seconds (1950 epochs). Finally, for smoothness, interpolation was used to upsample the data by a factor of 20.

Data Comparisons

Figure 4 plots the C/A code chip shapes for 12 GPS SVs. Example limits on the transient response performance parameters are plotted for comparison. The limits were selected based on potential variations expected for all 32 GPS SVs. For Rise Time and Peak Time, these were 25ns and 45ns, respectively. As stated previously, the Settling Time was fixed at 180ns; however the variation about the amplitude A, is 10%. The Peak Overshoot Ratio was bounded at 35%.

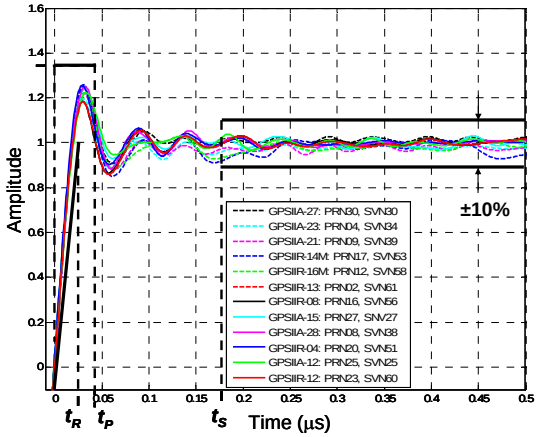

Figure 4. Comparison of the step responses on the C/A codes of 12 GPS SVs and the corresponding performance parameter limits.

To allow these nominal characteristics to be directly compared to second-order analog faults, a similar transient performance characterization was performed for the ICAO (analog) threat model. The damped natural frequency, F_D, was varied from 4 to 17 in 1-MHz increments. For each F_D, the damping parameter (σ) was varied from 0.8 to 8.8Mnepers/sec in increments of 0.5 MNepers/sec. Figure 5 shows the range of Rise Times for the ICAO analog faults; Figures 6 and 7 plot the Settling Times and PORs, respectively. Figure 8 summarizes the parameter limits for both nominal signals and deformed signals. Signals outside either of these can be characterized as "severely deformed."

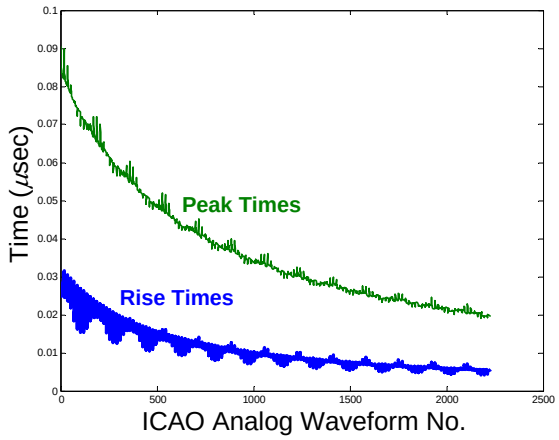

Figure 5. Rise Times and Peak Times for each of 2227 ICAO (analog-only) deformation threats

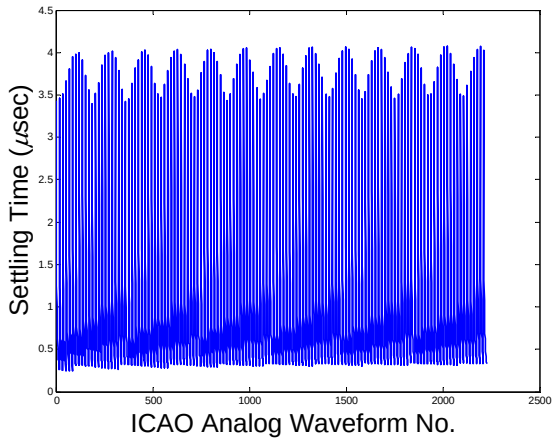

Figure 6. Settling Times for each of 2227 ICAO (analog-only) deformation threats.

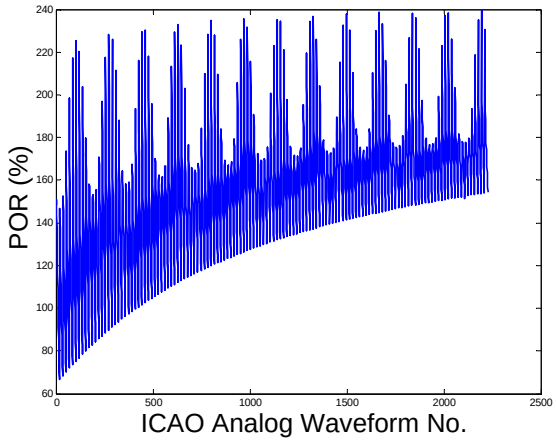

Figure 7. Peak Overshoot Ratios (%) for each of 2227 ICAO (analog-only) deformation threats. (Note: On this plot the POR for nominal signals would range from 0 to 35%)

Note that each region (with the exception of the "Severely Deformed Signals" region) leverages a specific characterization model. While many arbitrary signals can be conceived that are within the given parameter bounds, not every signal (e.g., an ideal, infinite bandwidth one) is realizable or is practical to consider. Deformed analog signals were analyzed as second-order step responses of the ICAO threat model. The nominal signals, however, are not second-order signals. They require a different modeling approach to adequately characterize them.

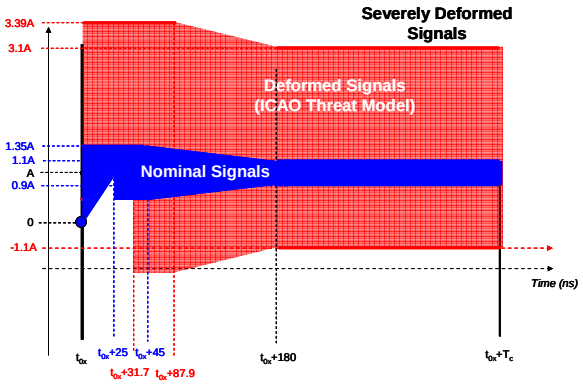

Figure 8. Summary of step response performance limits for all C/A code signals.

3. Model Nominal Waveforms

To analyze the potential receiver errors experienced by users of nominal signals meeting the desired performance specifications, a model for nominal signals must be derived. One straightforward approach for this is to infer the (unknown) model of the nominal filters from the (known) filter characteristics of second-order waveforms. This approach provides some continuity between the nominal and deformed regions of Figure 8. In addition, the filter model parameters themselves can provide some insights into potential hardware imperfections likely to translate into perturbations of the nominal signal.

Three specific filter characteristics were selected for variation. These included: resonant bandwidth, differential magnitude response, and differential group delay. The resonant bandwidth (BW_{res}) parameter corresponds to twice the resonant frequency of the second-order model (i.e., $2*F_D$). For the nominal signals, it is the traditional (double-sided) bandwidth of the filter. Intuitively, this parameter varies the frequency of the analog oscillations.

The maximum (passband) differential magnitude response ($[dH_{SD}]_{max}$) is the height of the peak passband magnitude response (in dB). This value is always positive for the highly oscillatory second-order waveforms. In general, changing this parameter varies the POR, Rise Times, and Peak Times of the signals.

The maximum (passband) differential group delay ($[dT_{Gd}]_{max}$) is the height of the peak passband group delay response (in ns). This parameter varies the phase of the nominal waveform. In combination with the differential magnitude response, this parameter also modifies the Settling Times as well.

The remaining parameters of the model, including filter rolloff, symmetry, etc. were fixed. Two ICAO analog model waveforms were used as an initial approximation for the nominal model parameter (and constant) selection. After some tuning, a compromise was reached between correspondence with the second-order waveforms outside of the nominal range and waveforms which approximate measured SV signals. The model equations are presented below.

For all frequencies f, when $f \le \left|\frac{BW_{res}}{2}\right|$, the model filter passband magnitude response was approximated by

$$H_{SD} = \frac{[dH_{SD}]_{max}}{\left(\frac{BW_{res}}{2}\right)^{H_{exp,inner}}} f^{H_{exp,inner}} \quad (1)$$

and the passband maximum differential group delay is

$$dT_{Gd} = \frac{[dT_{Gd}]_{max}}{\left(\frac{BW_{res}}{2}\right)^{T_{exp,inner}}} f^{T_{exp,inner}} \quad (2)$$

where $H_{exp,inner} = 2$ and $T_{exp,inner} = 6$.

Outside of the passband, when

$$\frac{BW_{res}}{2} \le f \le f_{max} \text{ or } \frac{BW_{res}}{2} \ge f \ge -f_{max} \quad (3)$$

Equations (1) and (2) become

$$H_{SD} = \frac{[dH_{SD}]_{max} + |H_{SD,min}|}{\left(f_{max} - \frac{BW_{res}}{2}\right)^{H_{exp,outer}}} (f \pm f_{max})^{H_{exp,outer}} - H_{SD,min} \quad (4)$$

and

$$dT_{Gd} = \frac{[dT_{Gd}]_{max}}{\left(f_{max} - \frac{BW_{res}}{2}\right)^{T_{exp,outer}}} (f \pm f_{max})^{T_{exp,outer}} \quad (5)$$

where $H_{SD,min} = -40$, $H_{exp,outer} = 6$, $T_{exp,outer} = 4$. In each of the above equations, $f_{max} = 40 + \left(\frac{BW_{res}}{2} - f_{d,min}\right)$ where $f_{d,min} = 4\text{MHz}$, corresponding to the minimum analog frequency in the ICAO model.

Figures 9 and 10 compare the filter responses of the two selected ICAO analog waveforms (F_D=17MHz,

σ=0.8MNepers/sec and F_D=4MHz, σ=8.8MNepers/sec) and the new, approximated filter characteristics. For the model, the tunable parameter values were

$$BW_{res} = 8\text{MHz}, \left[dH_{SD}\right]_{\max} = 15.7\text{dB}, \left[dT_{SD}\right]_{\max} = 113.6\text{ns} \quad (6)$$

and

$$BW_{res} = 34\text{MHz}, \left[dH_{SD}\right]_{\max} = 23.95\text{dB}, \left[dT_{SD}\right]_{\max} = 1060\text{ns} \quad (7)$$

for the low-frequency and high-frequency waveforms, respectively. A comparison of each of the corresponding time-domain waveforms is given in Figures 11 and 12.

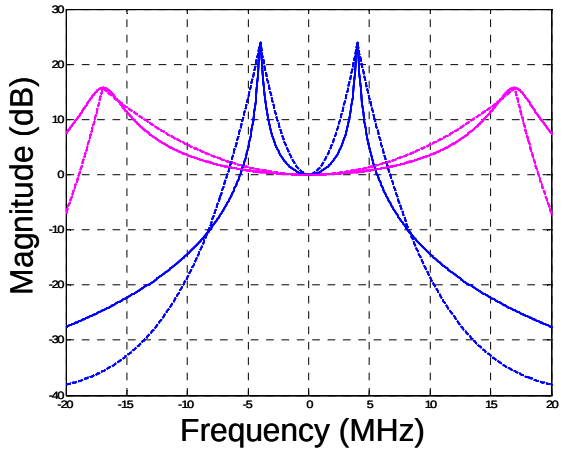

Figure 9. Comparison of actual (solid) and approximated (dashed) magnitude responses for two ICAO analog waveforms. (MAGENTA: F_D=17MHz, σ=0.8MNepers/sec; BLUE: F_D=4MHz, σ=8.8MNepers/sec)

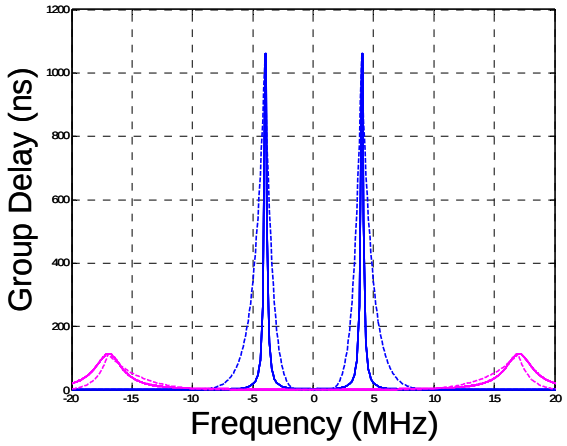

Figure 10. Comparison of actual (solid) and approximated (dashed) group delay responses for two ICAO analog waveforms. (MAGENTA: F_D=17MHz, σ=0.8MNepers/sec; BLUE: F_D=4MHz, σ=8.8MNepers/sec)

For the above parameterization, the approximation is better for the high-frequency waveform than the low-frequency one. This is expected. The nominal signals are high-frequency so the model constants are tuned to favor them. Of course, better approximations of any specific signal can be obtained by modifying some of the fixed parameters (e.g., $H_{exp,inner}$ and $H_{exp,outer}$) and by further tuning the variable ones.

A comparison of an approximated nominal waveform to an empirical model (i.e., an averaged nominal step response) is shown in Figure 13. Though not exact, the correspondence of the two traces is quite good. The proposed model computes nominal waveforms that can be varied within the range of the performance parameter limits previously depicted in Figure 8.

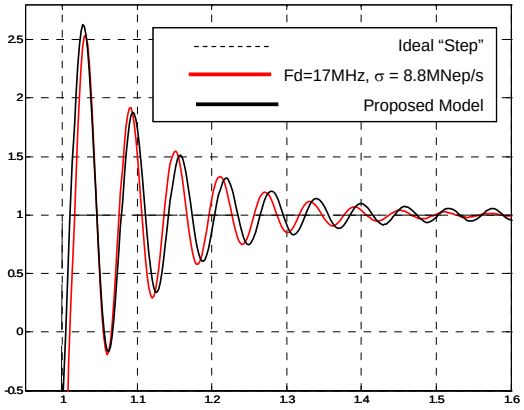

Figure 11. Comparison high-frequency ICAO waveform (F_D=17MHz, σ=0.8MNepers/sec) to proposed model approximation.

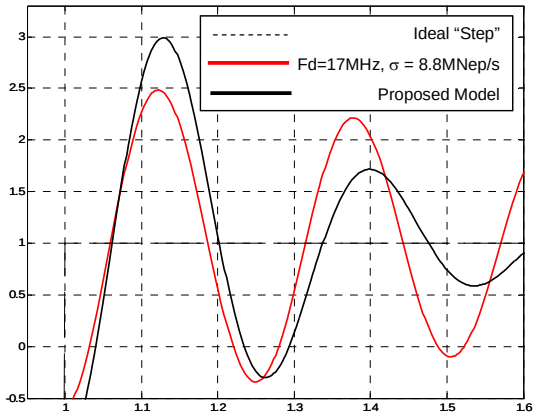

Figure 12. Comparison of high-frequency ICAO waveform (F_D=4MHz, σ=8.8MNepers/sec) to proposed model approximation.

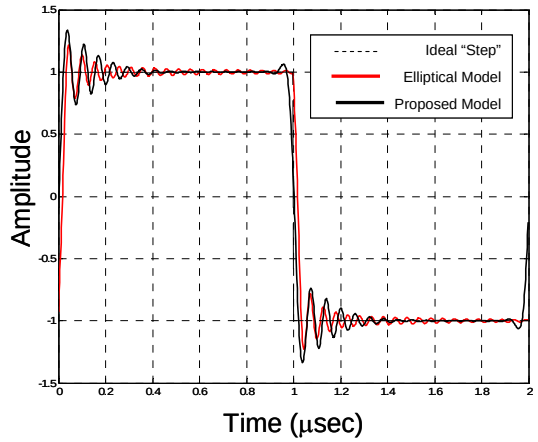

Figure 13. Comparison of an average nominal waveform (i.e., empirical model) to proposed model approximation.

4. Determine Worst Case User Receiver Errors

Once a wide range of suitable filter characterizations are determined from the model, each can be applied to PRN codes to create a wide range of nominally deformed signals. "Worst case" user receiver tracking errors can then be computed. (Here, worst-case implies that for any given receiver configuration, the nominal waveform which results in the smallest tracking errors is compared to the one that creates the largest errors.) The equations used for this analysis are described below.

The autocorrelation functions, $R(\tau)$, of each signal (at a delay offset, τ) can be modeled according to

$$R(\tau) = R_{USER}(\tau) = \int_{-\infty}^{\infty} H_{USER}(f)H(f)C(f)C_R^*(f)e^{j2\pi f}df \qquad (8)$$

where $H_{USER}(f)$ is the user receiver filter transfer function, $H(f)$ is the transfer function of the satellite signal filter. $C(f)$ and $C_R^*(f)$ represent the power spectra of the of the incoming code and the replica, respectively.

In Equation (8), $H(f)$ corresponds to the filter characterizations derived in the previous section. The user filter constraints ($H_{USER}(f)$) were dictated by specifications in the WAAS Minimum Operational Performance Standard (MOPS DO-229D) [7]. The form of the filter models were similar to the one represented by Equations (1) through (6); however, the decay of the magnitude response was prescribed to be 30dB per octave. Also, the maximum differential group delay parameter was varied between 0 and 150ns for receiver bandwidths above 7MHz wide. It was varied between 0 and 600ns for receivers between 2 and 7MHz.

Assuming coherent tracking and negligible phase error, the steady-state tracking error for a standard dot-product early-minus-late discriminator (with correlator spacing d chips) about the equilibrium point is given by

$$\tau = \arg\left\{R_{d(\bullet)}(\tau)\left[R_{d(\bullet)}\left(\tau - \frac{d}{2}\right) - R_{d(\bullet)}\left(\tau + \frac{d}{2}\right)\right] = 0\right\} \qquad (9)$$

The reference receiver had a correlator spacing d=1.0 chip. The filter was a high-quality SAW with nearly linear phase and 18MHz bandwidth. (This is the same filter used for the third example in [8].)

Given the above constraints, Figure 14 plots the nominal tracking errors for WAAS early-minus-late receivers. The errors are approximately 75cm for the wide bandwidth receivers with narrow correlator spacings. Intuitively, the errors are smallest (approximately 14cm) for these receivers with designs nearest that of the reference receiver configuration (18MHz, d=1.0 chips).

DISCUSSION

The tracking errors computed in Figure 14 represent the worst case nominal errors only for the assumptions, specifications, and constraints previously discussed. In particular, the assumed model for nominal waveforms is a key assumption that must accompany the parameter limits that are specified. The model presented here generates waveforms that are similar to the existing signals. (These signals are presumed to be operating as intentionally designed.) Note that many other waveforms—perhaps with vastly different model parameters—may exist within the nominal region presented here (in Figure 8) that can create user errors larger 75cm.

Once an appropriate model is chosen, however, the user errors that accompany them can be analyzed as previously shown. These errors, in turn, can be modified by implementing one or more of the following strategies:

- Changing the Rise Time, Peak Time, Settling Time, and/or POR limits.
- Changing the assumption of the reference correlator spacing and/or bandwidth.
- Modifying the constraints on the user receiver design space.

For future GNSS signals and systems, some combination of the above will likely be the most practical way of obtaining the best nominal user range accuracy.

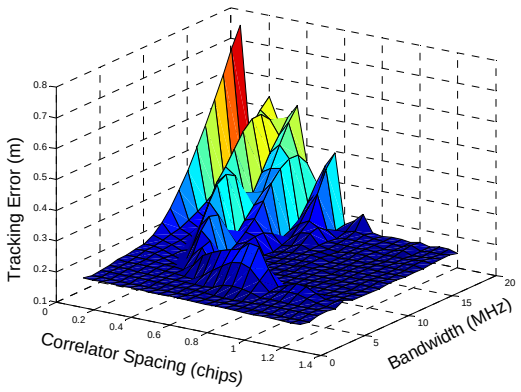

Figure 14. Example worst-case tracking errors due to nominal analog signal deformations on C/A code. (WAAS early-minus-late receivers modeled.)

CONCLUSIONS

A methodology for characterizing nominal analog signal deformations on GNSS signals was proposed. Step response performance criteria such as Peak Overshoot Ratio, Rise Time, Peak Time, and Settling Time criteria were used to set bounds on current GPS C/A code signal distortion performance assuming a nominal distortion model. High-resolution measurements of the signals of several GPS SVs were used to determine 35%, 25ns, 45ns, and 180ns (at 10% convergence), respectively.

A simple three-parameter filter model was proposed to model nominal signals throughout the full range of these parameter bounds. Based on these assumptions, the largest errors for standard early-minus-late users could range from 14cm to 75cm. These nominal range error estimates can be reduced for many by either tightening the specifications on the nominal signals coming from the satellite or by modifying the constraints placed on the reference and/or user receiver configurations.

Note, however, that different nominal signal models can produce different results. In order to bound the nominal errors with confidence, one must know the functional form the nominal signals can take.

ACKNOWLEDGMENTS

The authors would like to thank the Federal Aviation Administration for sponsoring this research under FAA Grant # CRDA 08-G-007. The opinions contained herein, however, are solely those of the authors.

REFERENCES

[1] Phelts, R.E., (2001) *Multicorrelator Techniques for Robust Mitigation of Threats to GPS Signal Quality*, Ph.D. Thesis, Stanford University, Stanford, CA.

[2] Edgar, C., Czopek, F., Barker, B., "A Co-operative Anomaly Resolution on PRN-19," *Proceedings of the 2000 13th International Technical Meeting of the Satellite Division of the Institute of Navigation, ION GPS-2000*. Proceedings of ION GPS 2000, v 2, pp. 2269-271.

[3] Mitelman, A.M., (2005) *Signal Quality Monitoring For GPS Augmentation Systems*, Ph.D. Thesis, Stanford University, Stanford, CA.

[4] Pini, M., Akos, D. "Analysis of GNSS Signals Using the Robert C. Byrd Green Bank Telescope," *Satellite Communications and Navigation Systems*. (Presentation.)

[5] Hegarty, C., Van Dierendonck, A. J., "Recommendations on Digital Distortion for the Civil GPS Systems", *Position Location and Navigation Symposium*, IEEE PLANS, May 2008, pp. 1090-1099.

[6] Hsu , P., Chiu, T., Golubev, Y., Phelts, R. E., "Test Results for the WAAS Signal Quality Monitor," *Proceedings of Position Location and Navigation Symposium*, IEEE/ION PLANS, 2008.

[7] Minimum Operational Performance Standards (MOPS) for WAAS, DO-229D. *RTCA*

[8] Phelts, R. E., "Sensitivity of Code Tracking Methods to PRN Differences," ENC-GNSS 2009.